HHS Public Access

Author manuscript

Genet Med. Author manuscript; available in PMC 2021 November 26.

Published in final edited form as:

Genet Med. 2021 September ; 23(9): 1624–1635. doi:10.1038/s41436-021-01182-1.

UBA2 variants underlie a recognizable syndrome with variable aplasia cutis congenita and ectrodactyly

Rhonda E. Schnur[#1,2,*], **Sairah Yousaf**[#3], **James Liu**[#3], **Wendy K. Chung**[4], **Lindsay Rhodes**[1], **Michael Marble**[5], **Regina M. Zambrano**[6], **Nara Sobreira**[7], **Parul Jayakar**[8], **Mary Ella Pierpont**[9], **Matthew J. Schultz**[10], **Pavel N. Pichurin**[10], **Rory J. Olson**[10], **Gail E. Graham**[11], **Matthew Osmond**[12], **Gustavo A. Contreras-García**[13], **Karina A Campo-Neira**[14], **Camilo A. Peñaloza-Mantilla**[14], **Mark Flage**[3], **Srikar Kuppa**[3], **Karina Navarro**[3], **Maria J. Guillen Sacoto**[1], **Ingrid M. Wentzensen**[1], **Maria I. Scarano**[2], **Jane Juusola**[1], **Carlos E. Prada**[15,16], **Robert B. Hufnagel**[3,*]

[1]Clinical Genomics Program, GeneDx, Gaithersburg, MD, 20877, USA

[2]Division of Genetics, Department of Pediatrics, Cooper Medical School of Rowan University, Cooper University Health Care, Camden, NJ, 08103, USA

[3]National Eye Institute, National Institutes of Health, Bethesda, MD, 20892, USA

[4]Division of Clinical Genetics, Departments of Pediatrics and Medicine, Columbia University, New York, NY, 10032, USA

[5]Department of Pediatrics, Division of Pediatric Genetics, University of New Mexico Health Sciences Center, Albuquerque, NM, 87106, USA

[*]Co-corresponding authors: Rhonda E. Schnur: rschnur@genedx.com, Robert B. Hufnagel: robert.hufnagel@nih.gov.

Author contributions:

RES and RBH designed and organized the study. SY and JL generated and analyzed zebrafish-related data. RES collated and composed sections describing human clinical data; SY and JL composed the core manuscript. RES and RBH supervised and validated data and reviewed and edited the manuscript. MF generated micro-computer tomography data. SK performed zebrafish genotyping and alcian staining. LR coordinated all clinical collaborations. RES, WKC, MM, RMZ, NS, PJ, MEP, MJS, PNP, RJO, GEG, MO, GACG, KAC, CAP, KN, MIS, CEP all contributed clinical patient information. MJGS, IMW, JJ analyzed exome data and provided clinical variant interpretations.

Declaration of Interests:

RES, IMW, MJGS, LR and JJ are employees of GeneDx, Inc., Gaithersburg, MD. The other authors declare no competing interests.

Ethics declaration:

Study participants were enrolled in approved protocols as per the policies of the Institutional Review Board Committees of the institutions at which patients were identified, or via GeneDx, following the tenets of the Declaration of Helsinki. The main IRB for this study is Western Institutional Review Board, Study Number 1175206, WIRB protocol # 20171030 (GeneDx). Written informed consent for inclusion in this study was obtained as required from all subjects, including specific consent to use photographs. All zebrafish-related experiments were conducted in accordance with recommendations of the Guide for the Care and Use of Laboratory Animals of the National Institutes of Health, protocol # NEI-679.

Web Resources:

ClinVar Database https://www.clinicalgenome.org/data-sharing/clinvar
gnomAD https://gnomad.broadinstitute.org/
GeneMatcher https://genematcher.org/
Pathogenicity predictions https://varsome.com/
OMIM http://www.omim.org/
Clustal omega https://www.ebi.ac.uk/Tools/msa/clustalo/

Supplemental Data

Supplemental data include a supplemental material and methods and results section, four figures and one table.

[6]Department of Pediatrics, Division of Genetics, Louisiana State University Health Sciences Center, New Orleans, LA, 70118, USA

[7]McKusick-Nathans Department of Genetic Medicine, Johns Hopkins University, Baltimore, MD, 21205, USA

[8]Division of Genetics and Metabolism, Nicklaus Children's Hospital, Miami, FL, 33155, USA

[9]Departments of Pediatrics and Ophthalmology, University of Minnesota Medical School, Minneapolis, MN, 55454, USA

[10]Department of Laboratory Medicine and Pathology, Mayo Clinic, Rochester, MN, 55905, USA

[11]Division of Genetics, Department of Pediatrics, Children's Hospital of Eastern Ontario, University of Ottawa, Ottawa, Ontario, K1H 8L1, Canada

[12]Children's Hospital of Eastern Ontario Research Institute, University of Ottawa, Ontario,K1H 8L1, Canada

[13]Division de Genética Médica, Departamento de Pediatría-Hospital Universitario de Santander, Departamento de Ciencias Básicas, Grupo de Investigación en Genética Humana UIS, Facultad de Salud, Universidad Industrial de Santander, Bucaramanga, Colombia

[14]Semillero de investigación en Genética Humana SIGENH, Escuela de Medicina, Facultad de Salud, Universidad Industrial de Santander, Bucaramanga, Colombia

[15]Department of Pediatrics, University of Cincinnati College of Medicine, Cincinnati, OH 45267 USA

[16]Division of Human Genetics, Cincinnati Children's Hospital Medical Center, Cincinnati, OH 45229 USA

[#] These authors contributed equally to this work.

Abstract

Purpose: The human chromosome 19q13.11 deletion syndrome is associated with a variable phenotype that includes aplasia cutis congenita (ACC) and ectrodactyly as specific features. *UBA2* (ubiquitin-like modifier-activating enzyme 2) lies adjacent to the minimal deletion overlap region. We aim to define the *UBA2*-related phenotypic spectrum in humans and zebrafish due to sequence variants and to establish the mechanism of disease.

Methods: Exome Sequencing was used to detect *UBA2* sequence variants in 16 subjects in 7 unrelated families. *uba2* loss-of-function was modeled in zebrafish. Effects of human missense variants were assessed in zebrafish rescue experiments.

Results: 7 human *UBA2* loss-of-function and missense sequence variants were detected. *UBA2*-phenotypes included ACC, ectrodactyly, neurodevelopmental abnormalities, ectodermal, skeletal, craniofacial, cardiac, renal, and genital anomalies. *uba2* was expressed in zebrafish eye, brain, and pectoral fins; *uba2*-null fish showed deficient growth, microcephaly, microphthalmia, mandibular hypoplasia, and abnormal fins. *uba2*-mRNAs with human missense variants failed to rescue nullizygous zebrafish phenotypes.

Conclusion: *UBA2* variants cause a recognizable syndrome with a wide phenotypic spectrum. Our data suggest that loss of *UBA2* function underlies the human *UBA2* monogenic disorder and highlights the importance of SUMOylation in the development of affected tissues.

Introduction

Features of the chromosome 19q13.11 deletion syndrome include early growth deficiencies, developmental delay, distinctive facial features, aplasia cutis congenita (ACC), hip dysplasia, digital and limb anomalies including ectrodactyly, and other malformations[1–8]. Deletions range in size from 1.37–11 Mb with a minimum overlapping region (MOR) of 324 kb, without clear genotype-phenotype correlation[3,4,6]. *UBA2* lies adjacent to the MOR and has been proposed to underlie key aspects of the deletion phenotype including ACC and ectrodactyly[1,2,3,5,6]. Limited patient data and lack of an animal model have prevented establishing *UBA2* as the causative gene.

UBA2 plays a key role in the posttranslational modification of protein (SUMOylation) by the addition of SUMO1 (small ubiquitin-like modifier) protein. UBA2 forms a heterodimer with SAE1 (SUMO-Activating Enzyme Subunit 1) and binds with SUMO1 in an ATP-dependent manner[9–11]. Unlike ubiquitination, SUMOylation does not only target proteins for degradation, but is involved in cell cycle regulation, subcellular trafficking, signal transduction, stress responses and chromatin structure dynamics. SUMOylation alters protein kinases and transcription factors to maintain transcriptional regulation of tissue-specific gene expression[12].

In this study, we report 16 additional individuals from seven unrelated families with *de novo* and familial *UBA2* sequence variants who have highly variable but overlapping clinical presentations. *In silico* modeling and a zebrafish *uba2* nullizygous phenotype provides further functional evidence for the pathogenicity of *UBA2* as the key gene underlying the chromosome19q13.11 microdeletion syndrome.

Material and methods

Subject enrollment and clinical evaluations

Each described patient was evaluated by a clinical geneticist. Written informed consent was obtained for exome sequencing either on a clinical or research basis. A written informed consent was also obtained from subjects to publish their photos. Genomic DNA was extracted from whole blood from affected probands and their biological parents for exome sequencing. See supplement for details.

Zebrafish modeling of the phenotypic effects of *uba2* variants

All animal experiments were conducted in accordance with recommendations of the Guide for the Care and Use of Laboratory animals of the National Institutes of Health (Protocol # NEI-679). Adult AB (Tubingen) and ABTL (Tubingen long fin) zebrafish strains were raised and maintained according to standard protocols as described[13].

Whole mount in situ hybridization

Wild type (WT) zebrafish embryos at different developmental stages (5 somite, 24, 35, 48, 72hpf (hours post fertilization), 5 and 7 dpf (days post fertilization) were fixed in preparation for performing in situ hybridization. See supplement method section for details.

CRISPR/Cas9 uba2 knock out line generation

CRISPR/Cas9 method was used to generate *uba2* knockout zebrafish lines. See supplement method section for details.

mRNA rescue

To evaluate the impact of human *UBA2* variants on encoded protein products, we utilized *uba2*-mutant fish to perform rescue studies with capped full-length human WT and missense alleles in mRNA transcribed with the T7 mMESSAGE mMACHINE kit (Ambion).

Please see supplement for other methodology details.

Results

Clinical studies

The cohort was gathered through GeneDx, a clinical molecular laboratory, and GeneMatcher. Investigators independently ascertained families with related phenotypes and rare candidate variants. Table 1 and the supplement contain additional clinical details.

Family 1: Family 1 (Fig. 1 and 2) is comprised of an affected mother and her four offspring. Two children have ACC. By report, the maternal grandmother and great grandmother also have histories of ACC. Other ectodermal changes are variable including thin scalp hair, xerosis and dental anomalies. The index case (IV-4, Fig. 1a and 1b) has unilateral ectrodactyly of hand. All of the other affected examined individuals have more subtle digital variations including camptodactyly, syndactyly, clinodactyly and diminished distal flexion creases of the fingers. All affected individuals share a high anterior hairline and mild frontal bossing, and several, including the proband (IV-4), have slightly down-slanted palpebral fissures. All have had highly variable neurodevelopmental problems, ranging from hypotonia to autism spectrum disorder in two of the brothers. Hypotonia generally persisted throughout childhood. Affected individuals had early growth deficiencies that improved with age. See supplement for other details. All affected individuals studied are heterozygous for a *UBA2* frameshift variant: c.816_817delAT, p.Trp273Alafs*13.

Family 2: This family consists of three affected brothers (Fig. 1b: II-1, II-2, II-3); neither parent is affected. Parentage was genetically confirmed prior to exome sequencing. All affected individuals have histories of hypotonia through childhood that impeded motor development and even feeding ability in early infancy, and sensory integration problems, but normal cognitive abilities. Neither ACC nor other ectodermal changes are noted, but the youngest brother (II-3) has unilateral cleft hand and polydactyly. More subtle foot, toe, and other minor digital anomalies vary among the three affected males. All three also have histories of cryptorchidism and/or hypospadias. Each is heterozygous for a "*de novo*"

frameshift *UBA2* variant, c.1376_1377insT, p.Thr460Aspfs*24, not detected in blood of either parent with either NextGen (130X coverage at 10X depth) or Sanger sequencing.

Family 3: Clinical details about part of this family were reported previously[14] but are now updated and expanded along with results of exome analysis. The male proband (II-2, Fig. 1a and 1b) has a single area of ACC, supernumerary nipple, cryptorchidism, early developmental delay, astigmatism, learning disability, depression, bipolar disorder, and social phobia. His mother (I-2) has multiple areas of healed ACC, supernumerary nipples, small head circumference, and asymmetric kidneys with reduced renal function. Neither have documented hand or foot anomalies. They are both heterozygous for a nonsense variant in *UBA2*: c.364C>T, p.Arg122*. Two other affected individuals (II-1 and III-1) have similar facial features, ACC, and supernumerary nipples and were each confirmed to harbor the familial *UBA2* variant.

Family 4: The female proband (II-1, Fig. 1b), 21 years old at examination, has a history of delayed motor skills and attention deficit disorder. Height, weight, and head circumference are all currently less than the third percentile; she also had early growth deficiency, delayed dentition and bone age. Features include ACC, thin scalp hair, clinodactyly, and overlapping toes. See Table 1 and supplement for additional endocrine, renal, and ophthalmologic concerns. She is heterozygous for a *de novo* missense variant in *UBA2,* c.167A>C: p.Asn56Thr.

Family 5: The female proband (Fig. 1b, II-1), 4 years and 9-months-old at exam, has developmental delay, absent speech, hemangiomas, ACC, and seizures. She has relative macrocephaly, epicanthal folds, anteriorly placed anus, and pes planus. She carries a *de novo* missense *UBA2* variant: c.1447G>A, p.Glu483Lys.

Family 6: The proband is a male toddler (Fig. 1a and 1b, II-1) with cryptorchidism, bilateral inguinal hernias, and multiple limb deformities including bilateral ectrodactyly of the feet, complete 2–3 finger syndactyly, clinodactyly and camptodactyly. He has low-normal growth and normal developmental milestones. Facial features include hypertelorism, bilateral epicanthal folds and pseudostrabismus. He does not have ACC or other ectodermal abnormalities. He is heterozygous for a *de novo UBA2* nonsense variant c.800T>A, p.Leu267*.

Family 7: The proband (Fig. 1b, II-1) is a 3 year 11-month-old Caribbean male born at 35 weeks gestational age. At two weeks, height and weight (corrected for prematurity) were normal, but head circumference measured at the 2nd centile. He had global developmental delay and four limb ectrodactyly, tall and prominent forehead, deep-set eyes, broad nasal root, left preauricular tag, narrow palate, and a vertical cleft chin. Pre-surgery, he had left 2–3 finger syndactyly with a nodule adjacent to the medial aspect of the PIP joint of the 4th finger. The right 3rd digit is missing; other digits are relatively normal. On the left foot, 2 malformed digits are divided by a deep central cleft; the right foot also has a deep central cleft with 3 malformed digits, and 4–5 toe syndactyly. He does not have ACC but has large areas of faint hypopigmentation over his torso and limbs. He is heterozygous for a *de novo* missense variant in *UBA2*: c.364C>G, p.Arg122Gly.

None of the detected *UBA2* variants was found in the GnomAD database[15]. Results of *in silico* predictor analyses for missense variants and variant classification is provided in Supplementary Tables 1 and 2. All would be classified as pathogenic or likely pathogenic using American College of Medical Genetics and Genomics (ACMG)/Association for Molecular Pathology (AMP) guidelines (classification criteria)[16] in Supplemental Table 2.

Modeling effects of missense variants on UBA2 function

UBA2 in complex with SAE1 plays a key role in the SUMOylation pathway. Observed human *UBA2* variants are distributed across the gene (Fig. 2a and b). All truncating variants are expected to undergo nonsense-mediated decay based on their position within the mRNA. Missense variants occur at residues that are strongly conserved across vertebrates (Fig. 2c). Given the similarities in phenotypes between individuals with truncating and missense alleles, we hypothesized that missense alleles also lead to loss-of-function.

To understand how missense alleles might disrupt UBA2 function, molecular modeling using published crystal structures[17] and simulated substitutions were performed for each detected human missense variant. In the UBA2 protein, p.Gly24[18] is directly involved in ATP binding; its substitution with valine results in altered protein conformation and is predicted to result in loss of ATP binding and ectopic interactions with nearby residues (Fig. 2d)[17]. Similarly, asparagine replacement with threonine at position 56 putatively abolishes ATP-dependent activation. The p.Arg122Gly substitution is predicted to result in loss of interaction with ATP. Human UBA2 protein interacts with a conjugating enzyme called UBC9 (amino acids 6–38) via amino acid residues 478–509, which include Glutamate 483. UBA2 forms a hydrophobic bond with Leu6, Met36 and Leu38 of UBC9; replacing Glutamate 483 with Lysine is predicted to disrupt UBA2-UBC9 binding. In summary, missense alleles observed in patients with *UBA2*-associated syndrome are observed to occur at functionally critical residues and potentially disrupt ATP-binding, protein folding, or protein-protein interactions.

Zebrafish *uba2* expression in affected tissues

By whole mount in situ hybridization, *uba2* transcript was detected on the dorsoventral axis of 5-somite stage embryos (Fig. S1a and b). At later stages, *uba2* is expressed in developing brain, eye, craniofacial structures, and fins. At 24 hpf, *uba2* expression was restricted to the head region, including the eye and nervous system (Fig. S1c). At 35 hpf, prominent signal was observed in pectoral fins (arrows, Fig. S1d). At all other examined stages (48 and 72 hpf, 5 and 7 dpf), *uba2* mRNA signal localized to the head region, specifically brain, neural retina, and lens (Fig. S1e–h). Therefore, zebrafish *uba2* is expressed in some structures that are analogous to those affected in humans harboring deleterious *UBA2* variants.

Variable expressivity observed with *uba2* loss-of-function

uba2 knockout zebrafish lines were generated by CRISPR/Cas9-targeted deletion. The phenotype of homozygous fish was notable for failure to inflate swim bladders. At 5–8 dpf, we observed severe gross morphological defects in *uba2*$^{-/-}$ zebrafish (Fig. 3) including small eyes, hydrocephalus and craniofacial edema, ventrally-curved body axis, and uninflated swim bladder. Faint heartbeat and severe pericardial edema were observed in

41% of embryos (Fig. 3a and b). Edema became generalized at 8 dpf when most lethality was noted. To further examine the effect of *uba2* on zebrafish development, we calculated the survival rate of *uba2*$^{-/-}$ zebrafish which was significantly lower than control (WT) and heterozygous fish. *uba2*$^{-/-}$ zebrafish showed a mortality rate of approximately 50% at 8 dpf; however, 100% of mutant fish were dead by day 12 (Fig. 3d).

Nullizygous fish exhibited a wide phenotypic range. We observed a pair of normal extended pectoral fins in WT zebrafish versus *uba2*$^{-/-}$ fish, where pectoral fins were found to be short and upright-oriented (Fig. 3a) confirming *uba2* function in fish extremity development. WT zebrafish had thin lines originating from base to fin tips showing normal actinotrichia. In contrast, *uba2*$^{-/-}$ fish displayed collapsed (Fig. 3b, middle image) and irregular fin fold edges (Fig. 3b, last image).

To better characterize variable expression and the relationship between the zebrafish knockout and the human disorders, we quantified craniofacial (F), brain (B), pectoral fin (PF), tail fin (TF) and swim bladder (SB) defects. Defects at later stages of development were studied in *uba2*$^{-/-}$ fish bred from the same parent at 8 dpf, when approximately half the fish survive (n=32; Fig. 3c). Tissue-level malformations were observed in craniofacial structures (9.38%), brain size (90.6%), tail fin (25%), pectoral fin (100%) and swim bladder (93.75%) (Fig. 3c and as described below). Thus, across individual fish with similar genetic backgrounds, total *uba2* function loss recapitulates some tissue-level phenotypes and the variable expression observed in human *UBA2*-related phenotypes.

Neuronal reduction in *uba2* zebrafish

Tissue-level analysis was performed in zebrafish to elucidate abnormalities resulting from *uba2* loss-of-function. First, we conducted immunohistochemistry studies on 8 dpf zebrafish cryosections through eye and brain. Compared to WT controls, *uba2*-null fish showed small heads, reduced midbrain size, low nuclei cell count with high accumulation of actin signal (orange, Fig. S2), implying a decreased proportion of gray to white matter. In addition, *uba2*$^{-/-}$ fish had smaller eyes, reduced retinal thickness, retinal laminations, and lens defects (see supplement).

Skeletal and extremity phenotypes in the *uba2* zebrafish model

To investigate the impact of *uba2* on zebrafish skeletal development, we stained *uba2* WT (+/+), heterozygous (+/−) and homozygous (−/−) fish with alcian blue dye at 5 dpf. In both *uba2* WT (Fig. 4a) and heterozygous zebrafish (data not shown), alcian staining demonstrated a normal pattern of cartilage element development including typical ceratohyoid, Meckel's cartilage, ceratobranchials arches and pectoral fin cartilage. However, complete loss of *uba2* in homozygous fish resulted in abnormal craniofacial development. In addition to jaw malformations, other craniofacial malformations included malformed and hypoplastic ventral and dorsal cartilage structures with lack of basihyal and hypohyal development. We also noted an apparently abnormal fusion of Meckel's cartilage with the palatoquadrate, resulting in a small, narrow mandible (Fig. 4b). Moreover, Meckel's cartilage was flattened at the midline fusion point with completely absent ceratohyal cartilage and ceratobranchials arches, the equivalent of micrognathia in these fish.

To explore whether *uba2* mutation causes skeletal phenotypes in adult fish, we performed micro-computed tomography (CT) comparing WT (n=3) and *uba2*$^{+/-}$ (n=3) fish, as nullizygous fish did not survive to this stage. We noted abnormal, wavy ribs and dysmorphic fin girdles in *uba2*$^{+/-}$ fish (Fig. S3).

In teleosts, finfolds are typically made of type II collagen matrix structures called actinotrichia that line the epidermis. Brightfield microscopy of *uba2*$^{-/-}$ fish revealed structural defects in median fins (Fig. 3b). To examine the effect of *uba2* truncation on zebrafish median fin structure development, we stained *uba2* zebrafish (+/+, +/− and −/−) larvae with type II collagen (Col2a) and Phalloidin (F-actin) antibodies to label actinotrichia (Fig. 4c).

Actinotrichia fibrils initiate fin development and become the future fin connective tissue. At 5 dpf, both WT (Fig. 4c, top panel) and heterozygous (data not shown) larvae develop median fins showed normally arrayed Col2a-labeled actinotrichia fibers; however, we observed non-rigid, non-parallel and bent actinotrichia in *uba2*−/− (Fig. 4c, arrows) fish. Phalloidin staining in *uba2*$^{-/-}$ fish revealed disorganized and disrupted organization, corresponding to areas of this abnormal collagen pattern (Fig. 4c).

Further investigating these extremity defects at a cellular level, we performed ultrastructural analysis of the *uba2* zebrafish body wall near the median finfold at 5 dpf. Detailed examination by TEM revealed a typical dynamically-assembled dense striated pattern of actinotrichia in WT fish (Fig. S4). Similarly, in WT fish we observed a normal and organized distribution of skeletal muscles with normal nuclei and mitochondria. However, in *uba2*$^{-/-}$ zebrafish, we observed disorganized (or incompletely developed) and scattered actinotrichia with abnormal epidermal cells (arrow). The skeletal muscle layer in homozygous fish was also observed to be discontinuous or atrophic with degenerated nuclei and mitochondria. Therefore, absent *uba2* impacts connective and epithelial tissue and skeletal muscle and causes extremity malformations in developing fish.

Conserved function of *UBA2* candidate variants in zebrafish

To further confirm the specificity of the *uba2* knockout phenotype, we attempted phenotypic rescue of developmental fish malformations by injecting human *UBA2* mRNA. Injected fish were grouped into three phenotypic classes and genotyped at 5 dpf, and the *uba2*$^{-/-}$ subset was analyzed. Embryos were classified as Class I (grossly normal body structure), Class II (decreased head size, absent swim bladder), and Class III (small head and body, generalized edema) (Fig. 4d). As compared to H_2O-injected controls, injecting human WT *UBA2* mRNA grossly rescued phenotypes in a significant number of fish. The proportion of Class I fish increased from 5% to 33%, and the proportion of Class III fish decreased from 47% to 6% ($p<0.0001$) (Fig. 4e). Even though WT-*UBA2* mRNA injection rescued gross phenotypes, most *uba2*$^{-/-}$ zebrafish still did not show inflated swim bladder (data not shown), suggesting that early *uba2* deficiency permanently impacts zebrafish physiology despite substitution with human mRNA.

Human mRNAs encoding p.Gly24Val, p.Arg122Gly and p.Glu483Lys all failed to rescue the *uba2*$^{-/-}$ phenotypes in contrast to WT mRNA. The p.Asn56Thr substitution demonstrated

statistically similar rescue to control mRNA; however, there were more Class III fish (23% vs 6%) and fewer Class I fish (18% vs 33%) following p.Asn56Thr injection, indicating possible partial loss-of-function for this missense substitution (Fig. 4e). Because the mRNAs containing the missense variants failed to rescue *uba2*-null phenotypes to a similar level as did WT *UBA2* mRNA, we conclude that the most likely mechanism of disease is loss-of-function.

Discussion

In this study, we describe a cohort of patients harboring deleterious variants in the *UBA2* gene. They show highly variable inter- and intra-familial expression of dermatologic, skeletal, extremity, neurologic, cardiac, and renal features, similar to those of the chromosome 19q13.11 microdeletion syndrome[1–8]. These observations further support *UBA2* as the critical gene in the microdeletion syndrome and suggest its essential role in early human growth and development. There are only a few other reports of intragenic *UBA2* variants (summarized in Table 1). Marble et al.[18] reported a de novo *UBA2* missense variant (c.71G>T, p.Gly24Val) in a 2.5-year-old female with ACC, thin hair, tall forehead, Duane anomaly, hip dysplasia, clinodactyly, and poor weight gain. Wang et al.[18] reported an inherited *UBA2* frameshift variant [c.327delT, p.Phe109Leufs*3] in a young boy and his mother. The mother had ACC but was otherwise healthy. The son had ACC, microcephaly, bilateral ectrodactyly, low-lying conus medullaris, horseshoe kidney and tracheoesophageal fistula. A *de novo UBA2* loss-of-function variant [c.1324dupT, p.Tyr442Leufs*17] was associated with four extremity split hand and foot malformation with tibial deficiency and under-masculinized external genitalia[19]. Aerden et al.[20] reported a male proband with ectrodactyly of the feet, autism spectrum disorder, craniofacial variations, dry sparse scalp hair, strabismus and hypermetropia who was heterozygous for a *de novo* frameshift variant in *UBA2* [c.612delA, p.Glu205Lysfs*63]; this was considered to be responsible for the phenotype[20].

The four patients previously reported with intragenic *UBA2* variants were added to our clinical summary table (Table 1) to compare phenotypes[18–21]. We've estimated the percentage of key traits in *UBA2* subjects (Fig. 1c) based on available clinical information. The most specific aspects of the *UBA2*-related phenotype are ACC, seen in 61%, and ectrodactyly, which is less common (37%). Early growth deficiency and neurodevelopmental delay are reported in 61% and 80% of affected individuals, respectively. More variable digital and skeletal abnormalities are also present (56%) but are sometimes subtle and potentially overlooked (e.g., Fig. 1a, panels C, D). These include clinodactyly (62%), syndactyly (59%), camptodactyly (57%), and hip abnormality (35%).The most common craniofacial variations are tall forehead/high hairline (76%), down-slanted palpebral fissures (47%), hypertelorism (62%), broad nasal root (81%), microcephaly (37%), and micrognathia (53%). Other observed features among our subjects include other ectodermal variations (~82%), ocular abnormalities (53%), cardiac (43%), genital (50%, in males) and renal (36%) abnormalities.

In *C. elegans, Uba-2* is also noted to be a critical element of the SUMOylation pathway; its ablation leads to embryonic lethality[22]. *UBA2* acute knockdown in xenograft

tumors by conditional shRNAs causes marked growth arrest, cell proliferation defects and increased apoptosis[23]. In mice, loss of any key component of the SUMOylation pathway can lead to severe impairment of cellular functions and lethality[24,25]. An in-situ hybridization study conducted in mouse embryos (8.5 to 11.5 days post-coitum) revealed *Uba2* ample expression at multiple morphogenetic activity sites, e.g. neural folds, branchial arches and limb buds[24], suggesting that *Uba2* is essential for normal cellular function/development. Recently, SUMOylation was reported to regulate differentiation of several ocular tissues[26,27].

Phenotypic features in our human *UBA2*-related syndrome cohort and the *uba2* knockout zebrafish are reminiscent of disorders associated with pathogenic variants in *DLX5/6* (split-hand/foot malformation (SHFM1, OMIM: 220600), *TP63* (e.g., Ectrodactyly, ectodermal dysplasia, and cleft lip/palate syndrome 3, EEC3, OMIM: 604292, split hand/foot malformation syndrome 4, SHFM4, OMIM: 605289 and others) and *FBXW4,* a candidate for SHFM3 (OMIM: 246560). *tp63*$^{-/-}$ zebrafish embryos have ectodermal defects involving skin, absent pectoral fin buds and reduced size fin folds at 36hpf and embryos died between 40–50hpf[28]. *tp63* zebrafish morphants affect skin integrity by making the skin more prone to microbial infection[29]. *fndc3a*$^{-/-}$zebrafish show broken actinotrichia, aberrant collagen localization and cellular defects in epidermal cells during caudal fin development[30]. It is possible that these genes function downstream of the SUMOylation pathway, leading to phenotypes that overlap the *UBA2*-related syndrome.

In the current study, the mRNA rescue experiments showed that WT-*UBA2* mRNA injection partially rescued the abnormal head/eye, tail, and uninflated swim bladder phenotype in *uba2*$^{-/-}$ zebrafish (33%). Notably, three of four human missense *UBA2* mRNAs did not rescue the *uba2*$^{-/-}$phenotype to a significant degree, suggesting a loss-of-function mechanism for these disease-associated alleles. As wide phenotypic variability is observed in both fish and human *UBA2*/*uba2*-related phenotypes, additional studies are warranted to define potential modifiers. Morpholinos (MOs) have been used in reverse genetic studies in a range of animal models[31,32]. However, MOs may be hard to interpret as they typically result in more severe phenotypes[33]. mRNA rescue in CRISPR-generated stable mutant lines are potentially useful in the interpretation of MO-related inconsistencies. Precise single nucleotide variant animal models of human diseases can help to better understand underlying molecular processes and may aid in management of *UBA2*-related abnormalities[34].

In conclusion, we report clinical details in 16 individuals from seven unrelated families with inherited or *de novo* heterozygous *UBA2* sequence variants, who present with highly variable phenotypes. Definition of the *UBA2*-related autosomal dominant phenotypic spectrum in humans, *in silico* modeling predictions, *uba2* expression and characterization of the knock out phenotype in zebrafish support the significance of *UBA2/uba2* in development, potentially by affecting post-translational modification of SHFM-associated genes. mRNA rescue experiments in zebrafish also suggest that loss of gene function is the primary mechanism of disease. The highly variable expressivity of the human *UBA2* phenotype, either via sequence alteration or contiguous gene deletion, even within the same family, remains incompletely explained; there are likely other modifiers, still

to be identified. However, our studies define a human disorder associated with *UBA2* sequence variants with a phenotype that overlaps key aspects of the chromosome 19q13.11 microdeletion syndrome.

Supplementary Material

Refer to Web version on PubMed Central for supplementary material.

Acknowledgments:

We gratefully thank the individuals and families who participated in this project. We would like to express our deepest gratitude to Dr. Mary Ella Pierpont for her valuable contribution and dedicate this report to her memory. WKC received financial support from the JPB Foundation. NR's work is supported by NHGRI grant 1U54HG006542. We would like to thank Dr. Sunit Dutta (National Eye Institute, NIH, Bethesda) for assistance in establishing *uba2* zebrafish knock out lines. We thank the Zebrafish facility, Confocal, transmission electron microscopy and micro-computed tomography mouse imaging facilities at NIH for their support and technical assistance. The research work carried out at NIH was supported by funds provided by National Eye Institute, National Institutes of Health, Bethesda, MD.

Data availability:

All data is mentioned in the main text and supplement, available to readers.

References

1. Abe KT, Rizzo I, Coelho ALV, Sakai N Jr., Carvalho DR, Speck-Martins CE. 19q13.11 microdeletion: Clinical features overlapping ectrodactyly ectodermal dysplasia-clefting syndrome phenotype. Clin Case Rep. 2018;6:1300–1307. [PubMed: 29988626]
2. Chowdhury S, Bandholz AM, Parkash S, et al.Phenotypic and molecular characterization of 19q12q13.1 deletions: a report of five patients. Am J Med Genet A. 2014;164A:62–69. [PubMed: 24243649]
3. Gana S, Veggiotti P, Sciacca G, et al.19q13.11 cryptic deletion: description of two new cases and indication for a role of WTIP haploinsufficiency in hypospadias. Eur J Hum Genet. 2012;20:852–856. [PubMed: 22378287]
4. Malan V, Raoul O, Firth HV, et al.19q13.11 deletion syndrome: a novel clinically recognisable genetic condition identified by array comparative genomic hybridisation. J Med Genet. 2009;46:635–640. [PubMed: 19126570]
5. Melo JB, Estevinho A, Saraiva J, Ramos L, Carreira IM. Cutis Aplasia as a clinical hallmark for the syndrome associated with 19q13.11 deletion: the possible role for UBA2 gene. Mol Cytogenet. 2015;8:21. [PubMed: 25883683]
6. Schuurs-Hoeijmakers JH, Vermeer S, van Bon BW, et al.Refining the critical region of the novel 19q13.11 microdeletion syndrome to 750 Kb. J Med Genet. 2009;46:421–423. [PubMed: 19487540]
7. Urquhart JE, Williams SG, Bhaskar SS, Bowers N, Clayton-Smith J, Newman WG. Deletion of 19q13 reveals clinical overlap with Dubowitz syndrome. J Hum Genet. 2015;60:781–785. [PubMed: 26377242]
8. Venegas-Vega C, Nieto-Martinez K, Martinez-Herrera A, et al.19q13.11 microdeletion concomitant with ins(2;19)(p25.3;q13.1q13.4)dn in a boy: potential role of UBA2 in the associated phenotype. Mol Cytogenet. 2014;7:61. [PubMed: 25516771]
9. Desterro JM, Rodriguez MS, Kemp GD, Hay RT. Identification of the enzyme required for activation of the small ubiquitin-like protein SUMO-1. J Biol Chem. 1999;274:10618–10624. [PubMed: 10187858]
10. He P, Sun X, Cheng HJ, et al.UBA2 promotes proliferation of colorectal cancer. Mol Med Rep. 2018;18:5552–5562. [PubMed: 30387828]

11. Olsen SK, Capili AD, Lu X, Tan DS, Lima CD. Active site remodelling accompanies thioester bond formation in the SUMO E1. Nature. 2010;463:906–912. [PubMed: 20164921]
12. Chang SC, Ding JL. Ubiquitination and SUMOylation in the chronic inflammatory tumor microenvironment. Biochim Biophys Acta Rev Cancer. 2018;1870:165–175. [PubMed: 30318471]
13. Westerfield MThe zebrafish book : a guide for the laboratory use of zebrafish (Danio rerio). [Eugene, OR]: M. Westerfield; 2007.
14. Marble M, Pridjian G. Scalp defects, polythelia, microcephaly, and developmental delay: a new syndrome with apparent autosomal dominant inheritance. Am J Med Genet. 2002;108:327–332. [PubMed: 11920840]
15. Lek M, Karczewski KJ, Minikel EV, et al.Analysis of protein-coding genetic variation in 60,706 humans. Nature. 2016;536:285–291. [PubMed: 27535533]
16. Richards S, Aziz N, Bale S, et al.Standards and guidelines for the interpretation of sequence variants: a joint consensus recommendation of the American College of Medical Genetics and Genomics and the Association for Molecular Pathology. Genet Med. 2015;17:405–424. [PubMed: 25741868]
17. Lois LM, Lima CD. Structures of the SUMO E1 provide mechanistic insights into SUMO activation and E2 recruitment to E1. EMBO J. 2005;24:439–451. [PubMed: 15660128]
18. Marble M, Guillen Sacoto MJ, Chikarmane R, Gargiulo D, Juusola J. Missense variant in UBA2 associated with aplasia cutis congenita, duane anomaly, hip dysplasia and other anomalies: A possible new disorder involving the SUMOylation pathway. Am J Med Genet A. 2017;173:758–761. [PubMed: 28110515]
19. Yamoto K, Saitsu H, Nishimura G, et al.Comprehensive clinical and molecular studies in split-hand/foot malformation: identification of two plausible candidate genes (LRP6 and UBA2). Eur J Hum Genet. 2019;27:1845–1857. [PubMed: 31332306]
20. Aerden M, Bauters M, Van Den Bogaert K, et al.Genotype-phenotype correlations of UBA2 mutations in patients with ectrodactyly. Eur J Med Genet. 2020:104009. [PubMed: 32758660]
21. Wang Y, Dupuis L, Jobling R, Kannu P. Aplasia cutis congenita associated with a heterozygous loss-of-function UBA2 variant. Br J Dermatol. 2020;182:792–794. [PubMed: 31587267]
22. Jones D, Crowe E, Stevens TA, Candido EP. Functional and phylogenetic analysis of the ubiquitylation system in Caenorhabditis elegans: ubiquitin-conjugating enzymes, ubiquitin-activating enzymes, and ubiquitin-like proteins. Genome Biol. 2002;3:RESEARCH0002. [PubMed: 11806825]
23. Carrington B, Varshney GK, Burgess SM, Sood R. CRISPR-STAT: an easy and reliable PCR-based method to evaluate target-specific sgRNA activity. Nucleic Acids Res. 2015;43:e157. [PubMed: 26253739]
24. Costa MW, Lee S, Furtado MB, et al.Complex SUMO-1 regulation of cardiac transcription factor Nkx2–5. PLoS One. 2011;6:e24812. [PubMed: 21931855]
25. Zhao JSumoylation regulates diverse biological processes. Cell Mol Life Sci. 2007;64:3017–3033. [PubMed: 17763827]
26. Nie Q, Xie J, Gong X, et al.Analysis of the Differential Expression Patterns of Sumoylation Enzymes E1, E2 and E3 in Ocular Cell Lines. Curr Mol Med. 2018;18:509–515. [PubMed: 30636610]
27. Gong X, Nie Q, Xiao Y, et al.Localization Patterns of Sumoylation Enzymes E1, E2 and E3 in Ocular Cell Lines Predict Their Functional Importance. Curr Mol Med. 2018;18:516–522. [PubMed: 30636611]
28. Santos-Pereira JM, Gallardo-Fuentes L, Neto A, Acemel RD, Tena JJ. Pioneer and repressive functions of p63 during zebrafish embryonic ectoderm specification. Nat Commun. 2019;10:3049. [PubMed: 31296872]
29. Lee H, Kimelman D. A dominant-negative form of p63 is required for epidermal proliferation in zebrafish. Dev Cell. 2002;2:607–616. [PubMed: 12015968]
30. Liedtke D, Orth M, Meissler M, et al.ECM alterations in Fndc3a (Fibronectin Domain Containing Protein 3A) deficient zebrafish cause temporal fin development and regeneration defects. Sci Rep. 2019;9:13383. [PubMed: 31527654]

31. Yousaf R, Ahmed ZM, Giese AP, et al.Modifier variant of METTL13 suppresses human GAB1-associated profound deafness. J Clin Invest. 2018;128:1509–1522. [PubMed: 29408807]

32. Yousaf S, Sethna S, Chaudhary MA, Shaikh RS, Riazuddin S, Ahmed ZM. Molecular characterization of SLC24A5 variants and evaluation of Nitisinone treatment efficacy in a zebrafish model of OCA6. Pigment Cell Melanoma Res. 2020;33:556–565. [PubMed: 32274888]

33. Stainier DYR, Raz E, Lawson ND, et al.Guidelines for morpholino use in zebrafish. PLoS Genet. 2017;13:e1007000. [PubMed: 29049395]

34. Prykhozhij SV, Berman JN. Zebrafish knock-ins swim into the mainstream. Dis Model Mech. 2018;11.

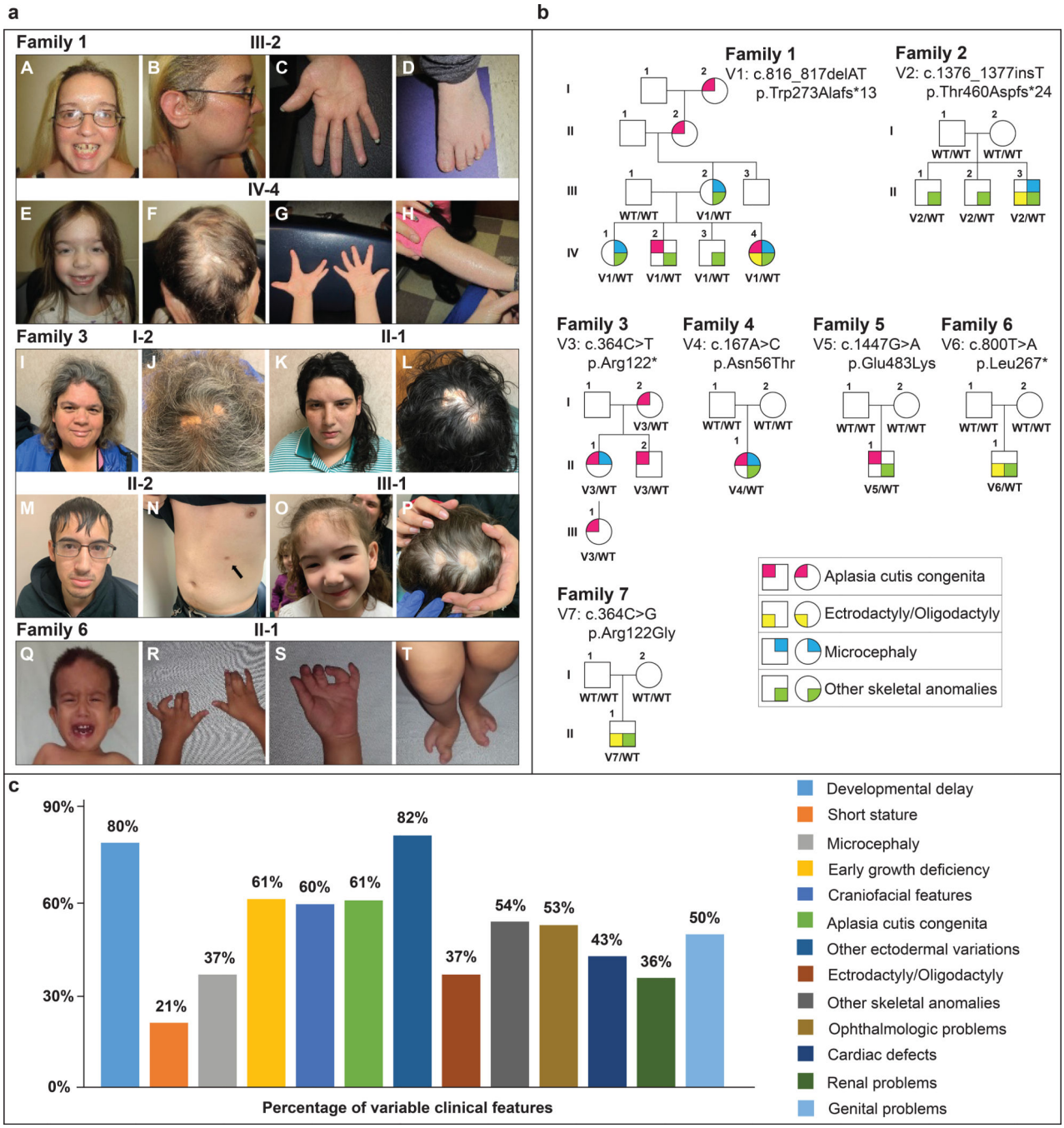

Figure 1: a. Clinical phenotypes and b. Pedigrees associated with *UBA2*-related syndrome.

a. Family 1, III-2: A. prominent forehead, high hairline, discolored peg-shaped teeth with gap between upper incisors, cleft chin B. low set ear with simple cartilaginous pattern C. diminished distal flexion creases D. brachydactyly, mild 2–3 syndactyly, clinodactyly of the 4th toe.

Family 1, IV-4: E. prominent forehead, high hairline, cleft chin, mildly down-slanted palpebral fissures F. ACC G. repaired ectrodactyly, hypoplastic distal flexion creases H. ichthyosis

Family 3, I-1: I. tall forehead, hypertelorism, broad nasal root, mild micrognathia J. ACC
Family 3, II-1: K. tall forehead, hypertelorism, broad nasal root, thin upper lip, medial eyebrow flare L. ACC
Family 3, II-2: M. facial features N. supernumerary nipple (arrow)
Family 3, III-1: O. tall forehead, low-set ears, micrognathia P. ACC
Family 6, II-1 Q. high forehead, hypertelorism, bilateral epicanthal folds R, S. bilateral 2–3 finger syndactyly, camptodactyly T. bilateral ectrodactyly of the feet

b. Affected individuals are shown as filled symbols. Genotypes are shown below each individual who was genotyped.

c. Percentages of different clinical features variably expressed in *UBA2*-affected individuals based on available data. Previously reported *UBA2* patients are also included in the percentages.

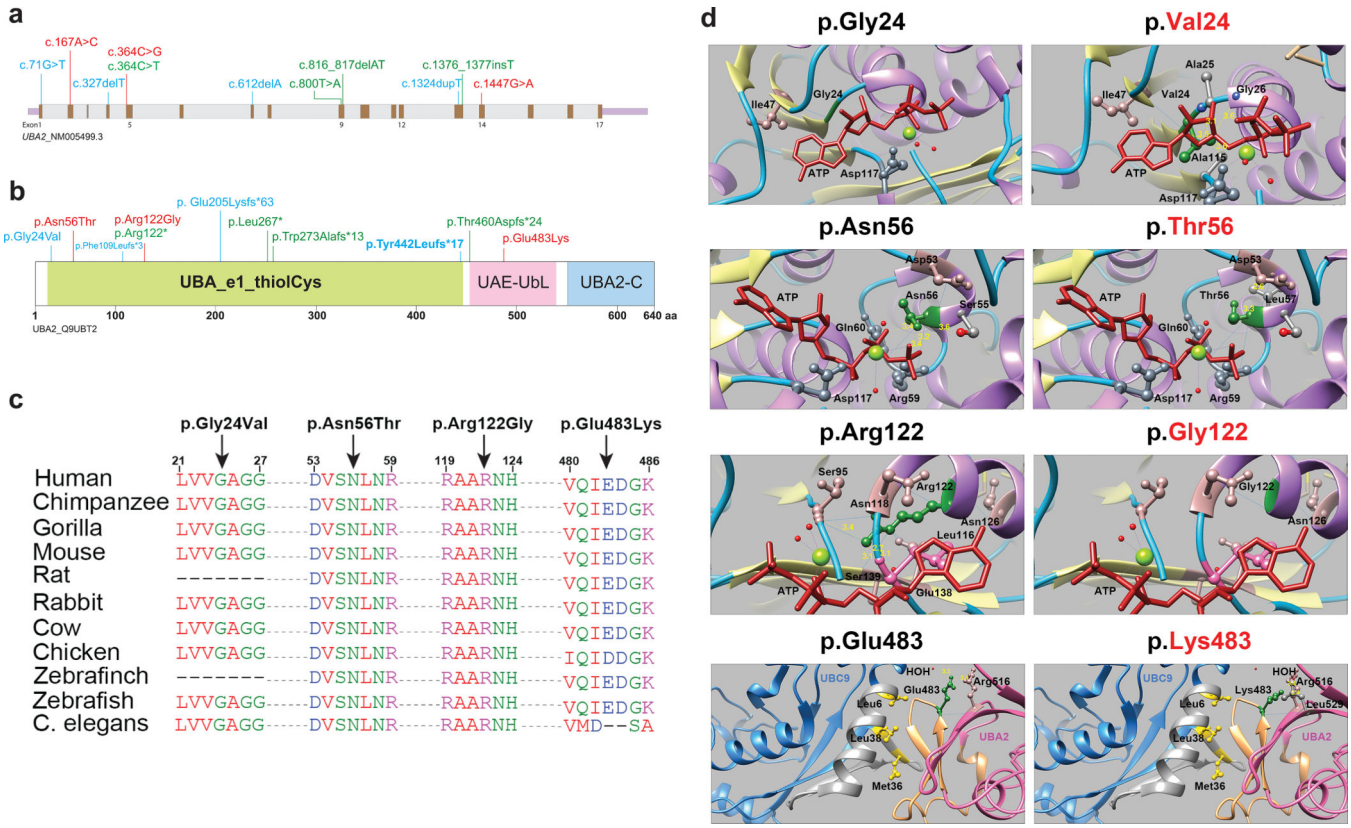

Figure 2: *UBA2* syndrome-associated variants and molecular modeling.

a. Schematic representation of the *UBA2* gene. Exons are shown in brown color boxes; introns and 3' and 5' UTRs are in light grey and purple, respectively. Newly reported *UBA2* missense and loss-of-function variants are shown in red and green, respectively, while blue is used to represent previously reported *UBA2* variants. b. Schematic representation of UBA2 protein domains. The UBA2 protein domain carrying catalytically active sites of ubiquitin-activating enzyme is shown in light green. This domain has putative active sites to bind ATP, substrate, and zinc with the last of five conserved cysteine residues playing an important role in ubiquitin thioester complex formation. UBA2-C (C-terminus) and UAE-UbL (ubiquitin-like) domains are shown in pink and blue, representing the C-terminus of UBA2 protein. UAE-UbL is structurally similar to ubiquitin and is involved in E1-SUMO-thioester transfer to E2 conjugation protein. The amino acid changes for the aforementioned variants are shown in the same color scheme as Figure 2B. c. Amino acid sequence alignments of the human UBA2 protein across different species at each of the residues reported with missense variants. d. Molecular modeling of human UBA2 protein. Secondary structure helix, strand and coil regions are shown in purple, yellow and cyan blue shades, respectively. Forest green color is used to show residues of interest in proteins with WT and missense changes and the ATP molecule is shown in brick red color. Blue color shows regions of hydrogen bonding and light pink shows residues involved in hydrogen bond formation with residues of interest. The distances to nearby residues are shown by dashed yellow lines. Last panel: UBA2 and UBC9 are shown in hot pink and cyan blue color, respectively. As per molecular modeling predictions, p.Gly24Val: Glycine is flexible enough to maintain torsion angles and is buried

in the protein core to maintain local secondary structure. p.Asn56Thr. Introducing a smaller but more hydrophobic residue at Asparagine 56 results in an empty space in the protein core and subsequent loss of hydrogen bonding with Asp53. p.Arg122Gly: The typical Arginine 122 residue is involved in hydrogen bonding with Asn118, Gly138 and Ser139. Replacement with Glycine is predicted to disrupt this array.

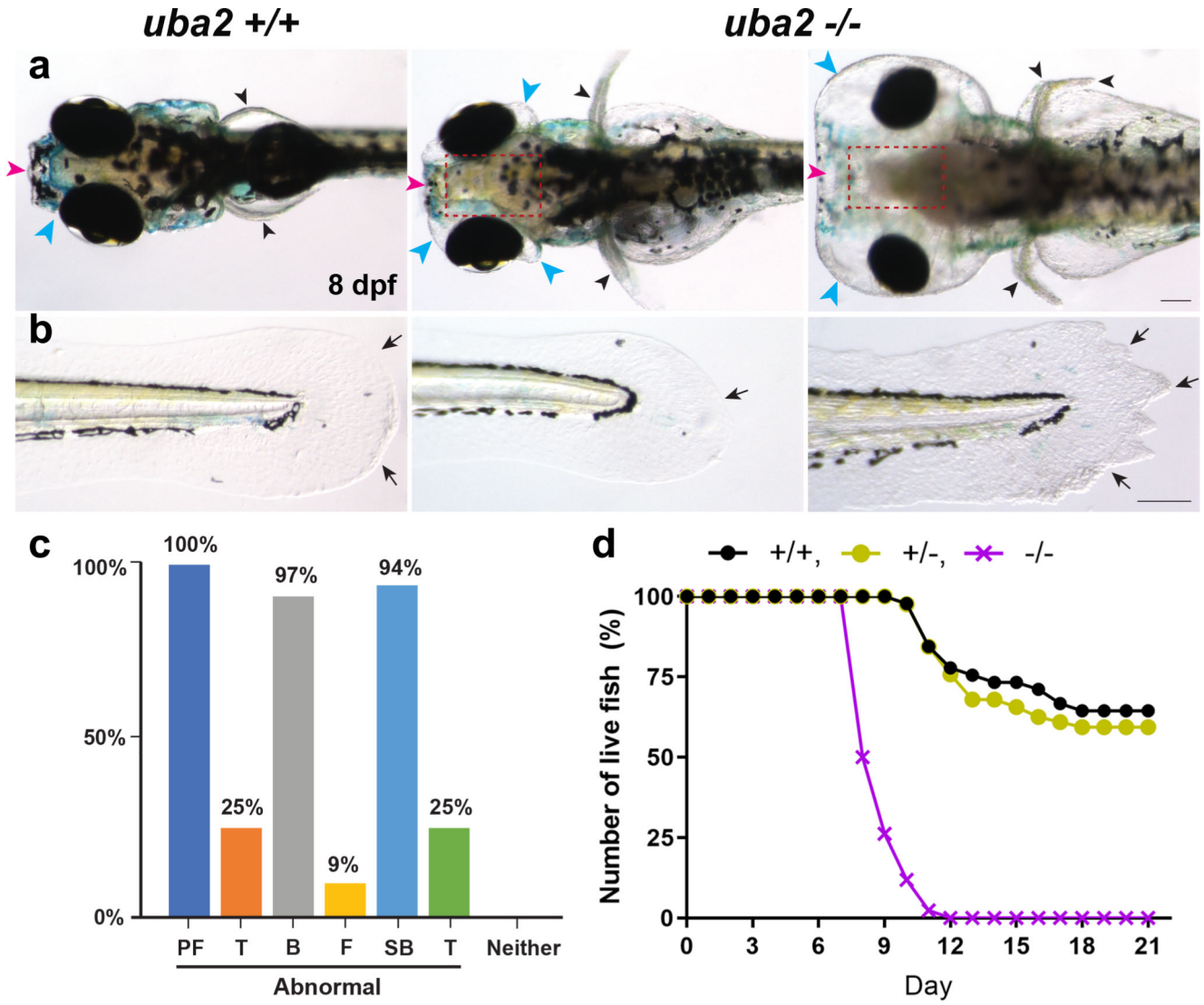

Figure 3: Severe dysmorphic features in embryonic *uba2*$^{-/-}$ zebrafish.

a-b. Dorsal and lateral views of *uba2* zebrafish at 8 dpf. Compared to WT controls, mutant lines showed aberrant head development with small eyes and hydrocephalus. c. Bar graph representing the percentage of *uba2*$^{-/-}$ zebrafish with gross morphological defects. d. Survival curve showing the number of live fish over the course of 21 days. WT and heterozygous fish showed similar death curves, but homozygous fish had steeper death curves with 100% mortality by day 12. PF (pectoral fins), T (tail), B (brain), F (craniofacial) and SB (swim bladder).

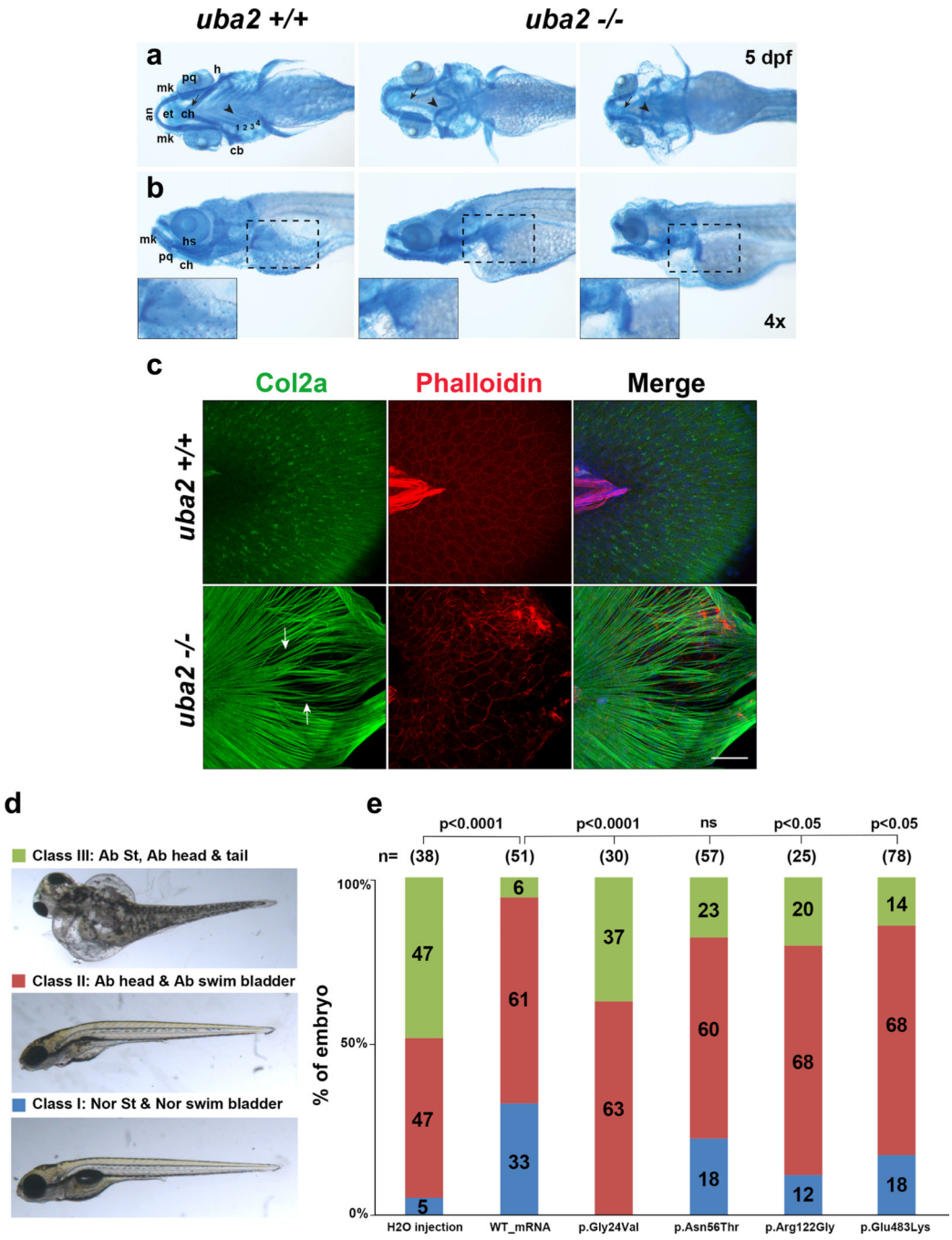

Figure 4: Cranial cartilage patterns observed in *uba2*$^{-/-}$ zebrafish and rescue of *uba2* mutant phenotype with human *UBA2* mRNA.

a-b. Brightfield ventral and lateral views of cartilage stained *uba2* in wild type and homozygous mutant fish are shown in top and bottom panels, respectively. Closeups of pectoral fin cartilage phenotype are shown in inserts in the bottom panel highlighted by black dashed boxes on lateral views. an (anterior), mk (Meckel's cartilage), pq (palatoquadrate), ep (ethmoid plate), ch (ceratohyal), h (hypohyal), cb (ceratobranchials 1–4), hs (hyosymplectic). c. Z-stack images of *uba2* zebrafish median fins stained with Col2a (green), Rhodamine-Phalloidin (red) and Dapi (blue). Arrows are used to show the

gaps between actinotrichia fibers. Scale bar: 50 μm. d. Suppression of *uba2* in zebrafish produces an abnormal phenotype which is classified into three categories. e. Proportions of *uba2*$^{-/-}$ zebrafish embryos representing each phenotype category after injecting with WT or mutation harboring human *UBA2* mRNA. Landmark abbreviations: Nor St (normal structure), Ab (abnormal) and ns (not significant). Chi Square test p-values are shown above the phenotypes for each rescue experiment.

Table 1:

us publications

Current age or age at exam (years)	Developmental delay/ neurodevelopmental details	Height percentile (most recent or at stated age)	Weight percentile (most recent or at stated age)	Head circumference percentile (most recent / stated age)	Early growth problems	Craniofacial features	Aplasia cutis congenita	Other ectodermal variations	Ectrodactyly/ Oligodactyly	Other skeletal anomalies	Other anomalies/ features: cardiac, renal, genital, ocular, miscellaneous	Other genetic/ chromosomal results
7	Normal development, but had behavior problems as child, history of seizures, mini strokes.	<5	increased	2		Tall forehead/ high hairline, hypertelorism, broad nasal root, facial asymmetry, cleft chin, ptosis, simple low set ears	no	Peg teeth, yellow teeth, thin hair, xerosis	no	Hypoplastic distal flexion creases, clinodactyly, syndactyly, camptodactyly, hip abnormality	Atrial fibrillation, mitral regurgitation by history but recent echo was normal. Hydronephrosis. Wears glasses. Focal nodular hyperplasia of the liver, hypofibrinogenemia.	Heterozygous for *FGG* LPATH variant: D344N. *WNT10B* heterozygous VUS: I285T.
5	Mild delays, hypotonia, has individualized educational plan, but she's academically on target.	25	67	2	Yes	Tall forehead/ high hairline, downslanted palpebral fissures, hypertelorism, broad nasal root, facial asymmetry, gap between incisors, slightly bifid uvula	no	Natal tooth, peg teeth, thin hair, eczema, keratosis pilaris, dental problems	no	Hypoplastic distal flexion creases, clinodactyly, syndactyly, camptodactyly, hip abnormality, scoliosis, pectus excavatum	ASD, aberrant right subclavian. Hydronephrosis/ pelviectasis, GU reflux, urinary tract infections. High myopia. Hypofibrinogenemia.	*FGG* heterozygous LPATH variant: p.D344N. Microarray: dup22q11.2.
3	Autism Spectrum disorder, behavior problems, encopresis, stereotypies, mood swings, hypotonia, normal MRI	26	66	20	yes	Tall forehead/ high hairline, downslanted palpebral fissures, hypertelorism, broad nasal root, facial asymmetry, triangular face, mild synophrys, telecanthus, cleft chin, micrognathia	yes, single area	Xerosis, thin hair, gaps between teeth, irregular enamel, supernumerary nipple, hyperhidrosis, hyperlinearity of palms, cutis marmorata, nail ridging, keratosis pilaris	no	Clinodactyly, syndactyly, camptodactyly, hip abnormality. Wore helmet for torticollis and plagiocephaly.	PFO (resolved). Astigmatism.	Normal CGH. Normal *MID1* sequencing.
	Autism Spectrum disorder, hypotonia, possible processing delay, poor coordination, MRI essentially normal	18	54	~30	yes	Tall forehead/ high hairline, orbital asymmetry, square uvula, ankyloglossia, cleft chin	no	Xerosis, keratosis pilaris, unruly hair, atopic dermatitis, history of heat exhaustion	no	Clinodactyly, syndactyly, camptodactyly, hip abnormality, wormian bones, mild pectus excavatum	PFO (resolved). Astigmatism. Hypofibrinogenemia.	*FGG* heterozygous LPATH variant: p.D344N.

Current age or age at exam (years)	Developmental delay/ neurodevelopmental details	Height percentile (most recent or at stated age)	Weight percentile (most recent or at stated age)	Head circumference percentile (most recent / stated age)	Early growth problems	Craniofacial features	Aplasia cutis congenita	Other ectodermal variations	Ectrodactyly/ Oligodactyly	Other skeletal anomalies	Other anomalies/ features: cardiac, renal, genital, ocular, miscellaneous	Other genetic/ chromosomal results
	Mild delays, intermittent intention tremor, brisk patellar reflexes, poor balance, hypotonia, normal cognitive skills, MRI normal.	11	11	~2	yes	Tall forehead/ high hairline, downslanted palpebral fissures, broad nasal root, facial asymmetry, low set ears, simple cartilage, wide uvula, cleft chin, micrognathia	yes, multiple areas	Xerosis, mild ichthyosis, keratoderma follicular prominence, thin dry hair, frayed toenails, hyperlinear palms, hypohidrosis.	yes, unilateral hand	Hypoplastic distal flexion creases, brachydactyly of toes, clinodactyly, syndactyly, camptodactyly, hip abnormality, mild pectus excavatum and hyperextensibility, wormian bones	PFO (resolved). Early myopia, -4 diopters, improved. History of “twisted optic nerves.” Hypofibrinogenemia, reduced IgA, IgM.	Normal SNP microarray. Normal *TP63* gene sequencing. *FGG* heterozygous LPATH variant: p.D344N. *WNT10B* heterozygous VUS: p.I285T.
1	Delays. Hypotonia, sensory integration problems, normal cognitive development	10	<3	~5	no	Tall forehead/ high hairline, downslanted palpebral fissures, broad nasal root, facial asymmetry, epicanthal folds, long and smooth philtrum, high arched palate, dental crowding	no	no	no	Long thin fingers, foot anomalies, clinodactyly, pectus excavatum, plagiocephaly	Cryptorchidism, hydrocele	
2	Delayed motor skills, hypotonia, sensory integration problems.	"low"		<5	yes	Downslanted palpebral fissures, broad nasal root, zygomatic arch hypoplasia, simple, low set posteriorly rotated ears, preauricular tag, long smooth philtrum, high arched palate, micrognathia	no	no	no	Dysplastic metatarsals, toes point outward, kyphoscoliosis	Hypospadias, inguinal hernia.	
	Delays, unstable gait, poor fine motor skills, sensory integration problems, poor balance, hypotonia, normal cognitive skills.	<3	<3	<3	yes	Normally set ears	not noted	no	yes, unilateral partial central cleft of hand, polydactyly of third finger	Syndactyly, camptodactyly	Cryptorchidism, hydrocele	46, XY and normal microarray

Current age or age at exam (years)	Developmental delay/ neurodevelopmental details	Height percentile (most recent or at stated age)	Weight percentile (most recent or at stated age)	Head circumference percentile (most recent / stated age)	Early growth problems	Craniofacial features	Aplasia cutis congenita	Other ectodermal variations	Ectrodactyly/ Oligodactyly	Other skeletal anomalies	Other anomalies/ features: cardiac, renal, genital, ocular, miscellaneous	Other genetic/ chromosomal results
5	Delays, learning difficulties in school, depression in adulthood.	<5	>95	~5–10		Tall forehead/ high hairline, hypertelorism, broad nasal root, low set prominent ears, thin vermilion border, mild micrognathia	yes, multiple areas	Supernumerary nipples	no	none reported	Recurrent urinary tract infections; asymmetric renal sizes with reduced function of smaller kidney. Hypothyroidism, s/p cholecystectomy. Inguinal herniorrhaphy. History of pseudotumor cerebri.	
4.5	Delays (walked at 17 months, first words at 22 months), special education, depression and anxiety as an adult.	~15	~93	<3rd		Tall forehead/ high hairline, hypertelorism, broad nasal root, thin upper lip, smooth philtrum, everted lower lip, thick, lowset, and laterally protruding ears, medial eyebrow flare, micrognathia	yes, 3 areas	Supernumerary nipple	no	none reported	Bicuspid aortic valve. Astigmatism. S/p cholecystectomy, migraines. Low back pain.	
1.5	Delays recognized at 16 months, learning difficulties and special education, bipolar disease, panic attacks and social phobias as an adult.	~20	~15	~60–70		Tall forehead/ high hairline, downslanted palpebral fissures, hypertelorism, broad nasal root, prominent columella, bulbous tip of the nose, micrognathia	yes, single area	Supernumerary nipple	no	none reported	Cryptorchidism. Astigmatism. Asthma.	
.75	Delays (at 16 months, cognitive function was at the 8 month old level, motor skills were at the 9 month level; at 30 months: still no sentences)	50	75–90	3–10	no	Tall forehead/ high hairline, downslanted palpebral fissures, hypertelorism, broad nasal root, lowset ears, micrognathia	yes, multiple areas	Supernumerary nipple	no	none reported	Frequent otitis. Constipation.	

Current age or age at exam (years)	Developmental delay/ neurodevelopmental details	Height percentile (most recent or at stated age)	Weight percentile (most recent or at stated age)	Head circumference percentile (most recent / stated age)	Early growth problems	Craniofacial features	Aplasia cutis congenita	Other ectodermal variations	Ectrodactyly/ Oligodactyly	Other skeletal anomalies	Other anomalies/ features: cardiac, renal, genital, ocular, miscellaneous	Other genetic/ chromosomal results
1	Delayed motor skills, attention deficit disorder, sat independently at 12 months, walked at 22 months, first word at 18 months, sentences after 2 years.	<3	<3	<3	yes	High hairline, broad forehead, hypertelorism, broad nasal root, delayed dentition, mild facial dysmorphism	yes	Thin, sparse hair, coarse skin, poor sweating, cries with tears.	no	Clinodactyly, overlapping toes on right foot (3,4), delayed bone age, kyphoscoliosis treated with bracing	Renal hypoplasia, chronic kidney disease, stable. Bilateral optic nerve hypoplasia with normal vision. Postural orthostatic hypotension. Hypothyroidism, growth hormone treatment, headaches, no breast development (budding only), menarche at 14 years, pubic hair, no axillary hair.	*BAZ1B*: heterozygous VUS, de novo fs c.3317delA; *SOS1:* heterozygous variant c.281T>C; *COX1:* homoplasmic p.I97V; *NRXN1:* heterozygous VUS, p.G744R (maternal)
.75	Global delay (gross motor and speech), nonverbal, refractory seizures, infantile spasms, hyperactivity, hypotonia.	~75	~10	~25	no	Epicanthal folds	yes	Normal hair and nails.		Pes planus	Hemangiomas (left ear, back). Anteriorly placed anus.	Normal microarray, normal Prader Willi/Angelman methylation, epilepsy panel: heterozygous VUS in *GABRB3*, paternal: p.R409Q
.5	Normal development	10–25	10–25	5–10	no	Tall forehead/ high hairline, hypertelorism, epicanthal folds, pseudostrabismus	no		yes, bilateral ectrodactyly of the feet	Clinodactyly, complete bilateral 2–3 finger syndactyly camptodactyly	Cryptorchidism. Bilateral inguinal hernias.	Normal SNP microarray
.9	Gross, fine motor and speech delays, persistent.	75–90	~75	25	no	Tall forehead/ high hairline, broad nasal root, left preauricular ear tag, narrow palate, vertical cleft/groove in chin	no	Diffuse patches of hypopigmentation.	4 limb ectrodactyly, oligodactyly of both feet	Syndactyly as part of ectrodactyly	VSD, not clinically significant	Normal prenatal microarray; normal WES at another clinical lab
.5	Delayed motor development, normal cognitive ability.	25–50	3rd	25–50	yes	Tall forehead/ high hairline, downslanted palpebral fissures, suspected hypertelorism and broad nasal root	yes, single large area	Thin hair in photos.	no	Clinodactyly, hip abnormality	Duane anomaly, strabismus. Recurrent otitis media, croup, tonsillitis.	

Current age or age at exam (years)	Developmental delay/ neurodevelopmental details	Height percentile (most recent or at stated age)	Weight percentile (most recent or at stated age)	Head circumference percentile (most recent / stated age)	Early growth problems	Craniofacial features	Aplasia cutis congenita	Other ectodermal variations	Ectrodactyly/ Oligodactyly	Other skeletal anomalies	Other anomalies/ features: cardiac, renal, genital, ocular, miscellaneous	Other genetic/ chromosomal results
									Bilateral ectrodactyly, oligodactyly, hands and feet	Clinodactyly, long bone deficiency of tibias	Undermasculinized external genitalia	
	Normal development	10–25 (birth)	<3 (birth)	<10 (birth)			Yes, two areas		Bilateral ectrodactyly, oligodactyly	Syndactyly as part of ectrodactyly, low lying conus medullaris	Horseshoe kidney, tracheo-esophageal fistula	Normal karyotype, microarray
5	Normal development						yes		no	none reported		
	Speech delay, normal motor milestones, learning difficulties, autism diagnosed at 8 years, intelligence quotient 76.	~25–50 (3.6 years)	~25 (3.6 years)	~20 (3.6 years)	yes	Retrognathia, low set and prominent ears, fullness of upper eyelids.		Supernumerary nipple, increased hair on back, dry, sparse scalp hair.	yes	Polydactyly with six metatarsals on right foot, multiple bony anomalies in feet, syndactyly of toes, normal hands, transient hip instability. Normal hands.	Strabismus, hypermetropia	